INTERNATIONAL JOURNAL FOR NUMERICAL METHODS IN FLUIDS, VOL. 11, 849–865 (1990)

FINITE ELEMENT SOLUTION OF FLOW BETWEEN ECCENTRIC CYLINDERS WITH VISCOUS DISSIPATION

J. H. C. DE ARAUJO, V. RUAS AND A. S. VARGAS*

*Departamento de Informática (*Departamento de Engenharia Mecânica), Pontifícia Universidade Católica do Rio de Janeiro, Rua Marquês de São Vicente, 225, Rio de Janeiro, Brazil*

SUMMARY

A computational study of viscous flow between two eccentrically rotating cylinders is presented in which the effect of viscous dissipation is taken into account. The space discretization is based on piecewise linear finite elements with velocity stabilization, while the method of characteristics is used for time integration. Numerical results illustrate the efficiency of the adopted approach.

KEY WORDS Finite elements Navier-stokes Rotating cylinders Viscous dissipation

1. INTRODUCTION

The flow of a viscous incompressible fluid between two rotating cylinders is a problem of great importance in fluid dynamics. In particular it has relevant applications in mechanical engineering such as the design of journal bearings extensively employed in rotating machines.

The flow patterns are known to vary sharply with the Reynolds number and, if the cylinders are eccentric, the strong non-linearity of the problem requires a true two-dimensional modelling of the flow. For this reason, numerical study of this kind of flow appears to be the best possibility nowadays, although in the past reasonable results have been obtained by more classical approaches by several authors, among which those given by Taylor[1] are probably the best known.

However, in such approaches, among other simplifications, it is assumed that the effects of viscous dissipation are negligible. Since the journal bearings of modern machines are required to rotate at drastically increasing speeds, the assumptions of such simplified models may lead to excessively erroneous project specifications data.

The main purpose of this work is to introduce a finite element model aimed at studying the complete set of time-dependent equations in two-dimensional space describing the behaviour of a fluid between two cylinders, including the equation for heat generation by viscous dissipation.

The non-linear fluid motion equation is approximated via the method of characteristics, while the coupling with the energy equation for the temperature is handled by means of a standard alternating direction technique.

An outline of the paper is as follows. In Section 2 we give a physical description of the problem with the corresponding equations. In Section 3 we describe the different numerical approaches, including a finite element discretization using a piecewise linear triangle with velocity stabilization. In Section 4 representative numerical results obtained by implementing the numerical schemes are given, followed by some conclusions in Section 5.

0271–2091/90/140849–17$08.50 *Received November 1989*

2. STATEMENT OF THE PROBLEM

We want to solve the problem of the motion of a Newtonian viscous incompressible fluid in the region Ω illustrated in Figure 1, described by its velocity field and pressure.

The inner cylinder is assumed to be rotating at constant speed with respect to the outer one. We assume a no-slip boundary condition for the velocity on both walls. The temperature of the fluid is assumed to be constant on the cylinders and its distribution is assumed to be governed by both conduction and convection, with a supplementary source of energy due to the effects of viscous dissipation. The following additional assumptions are incorporated into the formulation of the problem.

(i) The flow is laminar.
(ii) The gravitational force is negligible.
(iii) The viscosity varies with temperature only.
(iv) The heat capacity and the thermal conductivity of the fluid are constant.

The equations governing the phenomenon under study are:

momentum

$$\rho\left(\frac{\partial\tilde{u}}{\partial\tilde{t}}+\tilde{u}\frac{\partial\tilde{u}}{\partial\tilde{x}}+\tilde{v}\frac{\partial\tilde{u}}{\partial\tilde{y}}\right)=-\frac{\partial\tilde{p}}{\partial\tilde{x}}+2\frac{\partial}{\partial\tilde{x}}\left(\tilde{\mu}\frac{\partial\tilde{u}}{\partial\tilde{x}}\right)+\frac{\partial}{\partial\tilde{y}}\left[\tilde{\mu}\left(\frac{\partial\tilde{u}}{\partial\tilde{y}}+\frac{\partial\tilde{v}}{\partial\tilde{x}}\right)\right],$$

$$\rho\left(\frac{\partial\tilde{v}}{\partial\tilde{t}}+\tilde{u}\frac{\partial\tilde{v}}{\partial\tilde{x}}+\tilde{v}\frac{\partial\tilde{v}}{\partial\tilde{y}}\right)=-\frac{\partial\tilde{p}}{\partial\tilde{y}}+2\frac{\partial}{\partial\tilde{x}}\left(\tilde{\mu}\frac{\partial\tilde{v}}{\partial\tilde{y}}\right)+\frac{\partial}{\partial\tilde{x}}\left[\tilde{\mu}\left(\frac{\partial\tilde{v}}{\partial\tilde{y}}+\frac{\partial\tilde{v}}{\partial\tilde{x}}\right)\right]; \tag{1}$$

conservation of mass

$$\frac{\partial\tilde{u}}{\partial\tilde{x}}+\frac{\partial\tilde{v}}{\partial\tilde{y}}=0; \tag{2}$$

energy

$$\rho c\left(\frac{\partial\tilde{T}}{\partial\tilde{t}}+\tilde{u}\frac{\partial\tilde{T}}{\partial\tilde{x}}+\tilde{v}\frac{\partial\tilde{T}}{\partial\tilde{y}}\right)=k\left(\frac{\partial^2\tilde{T}}{\partial\tilde{x}^2}+\frac{\partial^2\tilde{T}}{\partial\tilde{y}^2}\right)+\tilde{\mu}\left\{2\left[\left(\frac{\partial\tilde{u}}{\partial\tilde{x}}\right)^2+\left(\frac{\partial\tilde{v}}{\partial\tilde{y}}\right)^2\right]+\left(\frac{\partial\tilde{u}}{\partial\tilde{y}}+\frac{\partial\tilde{v}}{\partial\tilde{x}}\right)^2\right\}; \tag{3}$$

where $(\tilde{x}, \tilde{y})$ are the Cartesian co-ordinates, $\tilde{\mu}$ is the dynamic viscosity, ρ is the density, k is the thermal conductivity and c is the heat capacity.

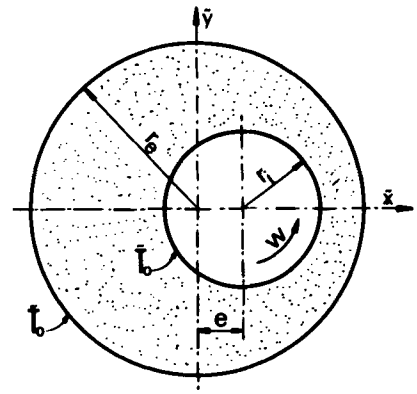

Figure 1. Schematic diagram of the problem

The dynamic viscosity is assumed to be a function of the temperature $\tilde{T}$ of the type

$$\tilde{\mu}(\tilde{T}) = A \exp\left(\frac{B}{\tilde{T}}\right), \tag{4}$$

where A and B are physical constants.

If we write

$$\tilde{x} = r_i x, \qquad \tilde{y} = r_i y, \qquad \tilde{t} = t/w,$$

$$\tilde{u} = uwr_i, \qquad \tilde{v} = vwr_i, \qquad \tilde{p} = p\rho(wr_i)^2, \qquad \tilde{T} = T\tilde{T}_0, \qquad \tilde{\mu} = \mu\tilde{u}_0,$$

$$Re = \frac{\rho w r_i^2}{\tilde{\mu}_0}, \qquad Pr = \frac{\tilde{\mu}_0 c}{k}, \qquad Pe = Pr\,Re, \qquad \lambda = \frac{w\tilde{\mu}_0}{\rho c \tilde{T}_0},$$

where $\tilde{\mu}_0 = \tilde{\mu}(\tilde{T}_0)$, equations (1)–(3) can be written in dimensionless form as

$$\frac{\partial u}{\partial t} + u\frac{\partial u}{\partial x} + v\frac{\partial u}{\partial y} = -\frac{\partial p}{\partial x} + \frac{1}{Re}\left\{2\frac{\partial}{\partial x}\left(\mu\frac{\partial u}{\partial x}\right) + \frac{\partial}{\partial y}\left[\mu\left(\frac{\partial u}{\partial y} + \frac{\partial v}{\partial x}\right)\right]\right\},$$

$$\frac{\partial v}{\partial t} + u\frac{\partial v}{\partial x} + v\frac{\partial v}{\partial y} = -\frac{\partial p}{\partial y} + \frac{1}{Re}\left\{2\frac{\partial}{\partial y}\left(\mu\frac{\partial v}{\partial y}\right) + \frac{\partial}{\partial x}\left[\mu\left(\frac{\partial u}{\partial y} + \frac{\partial v}{\partial x}\right)\right]\right\}, \tag{5}$$

$$\frac{\partial u}{\partial x} + \frac{\partial v}{\partial y} = 0, \tag{6}$$

$$\frac{\partial T}{\partial t} + u\frac{\partial T}{\partial x} + v\frac{\partial T}{\partial y} = \frac{1}{Pe}\left(\frac{\partial^2 T}{\partial x^2} + \frac{\partial^2 T}{\partial y^2}\right) + \mu\lambda\phi, \tag{7}$$

where

$$\phi = 2\left[\left(\frac{\partial u}{\partial x}\right)^2 + \left(\frac{\partial v}{\partial y}\right)^2\right] + \left(\frac{\partial u}{\partial y} + \frac{\partial v}{\partial x}\right)^2$$

is the dissipation function.

The boundary conditions to complete the system (5)–(7) are

$$t > 0 \begin{cases} (x - e/r_i)^2 + y^2 = 1 \to u = y,\ v = e/r_i - x,\ T = 1 \\ x^2 + y^2 = (r_e/r_i)^2 \to u = 0,\ v = 0,\ T = 1. \end{cases} \tag{8}$$

The initial conditions are

$$u = 0, \qquad v = 0, \qquad T = 1. \tag{9}$$

3. NUMERICAL MODELLING

In order to implement the method of characteristics, we first notice that the Navier–Stokes equations (5) and (6) can be written as

$$\frac{\mathbf{DV}}{\mathrm{D}t} = -\operatorname{grad} p - \frac{1}{Re}\operatorname{rot}(\mu \operatorname{rot} \mathbf{V}), \tag{10}$$

$$\operatorname{div} \mathbf{V} = \mathbf{0}, \tag{11}$$

where D/Dt denotes the material derivative.

Let us now introduce a time step Δt by means of which we perform a time discretization in system (10), (11) as follows.

We denote by $f^n(\mathbf{X})$ the approximation of a function $f(\mathbf{X}, t)$ for $t = n\Delta t$, $n \geqslant 0$.

Now we approximate the time derivative of f at time t, $n\Delta t \leqslant t \leqslant (n+1)\Delta t$, as

$$\frac{f^{n+1} - f^n}{\Delta t}.$$

Now we are given $\mathbf{V}^0$, $\mathbf{T}^0$ and we compute successively approximations $\mathbf{V}^{n+1}$, p^{n+1} and T^{n+1} for $n = 0, 1, 2, \ldots$ of the following alternating direction algorithm:

$$\frac{\mathbf{V}^{n+1}}{\Delta t} + \frac{1}{Re}\operatorname{rot}[\mu(T^n)\operatorname{rot}\mathbf{V}^{n+1}] = -\operatorname{grad} p^{n+1} + \frac{\mathbf{V}^n[\mathbf{X}^n(\cdot\,; t)]}{\Delta t}.$$

$$\operatorname{div}\mathbf{V}^{n+1} = \mathbf{0}, \tag{12}$$

$$\frac{T^{n+1}}{\Delta t} + \mathbf{V}^{n+1}\operatorname{div}[\operatorname{grad} T^{n+1}] - \frac{1}{Pe}\nabla^2 T^{n+1} = \mu(T^n)\lambda\phi(\mathbf{V}^{n+1}) + \frac{T^n}{\Delta t}, \tag{13}$$

where

$$\nabla^2 = \frac{\partial^2}{\partial x^2} + \frac{\partial^2}{\partial y^2}$$

and $\mathbf{X}(x, y, \tau; t)$ is the function which gives the position of a particle of the fluid at time τ, $n\Delta t \leqslant \tau \leqslant (n+1)\Delta t$.

On the other hand, given the position (x, y) of a particle at time t, its position at time τ is given by $\mathbf{X}(x, y, \tau; t)$, where

$$\frac{\mathrm{d}\mathbf{X}}{\mathrm{d}\tau} = \mathbf{V}^n[\mathbf{X}(x, y, \tau; t)]. \tag{14}$$

In the present framework we know $\mathbf{X}^{n+1}(\cdot\,; t)$ and we wish to calculate $\mathbf{X}^n(\cdot\,; t)$. In order to do so, we integrate backwards the above differential equation by a second-order Runge–Kutta method, thereby defining $\mathbf{X}^n(\cdot\,; t)$ as follows:

$$\mathbf{X}^n = \mathbf{X}^{n+1} - \frac{\Delta t}{2}\{\mathbf{V}^n(\mathbf{X}^{n+1}) + \mathbf{V}^n[\mathbf{X}^{n+1} - \Delta t\,\mathbf{V}^n(\mathbf{X}^{n+1})]\}. \tag{15}$$

Solution methods of equation (14) based on such an integration scheme are known to be unconditionally stable.[2] However, in order to determine quick variations of the velocity, it is highly advisable to use small time steps.

Notice that (12) is nothing but a Stokes system for $(\mathbf{V}^{n+1}, p^{n+1})$. As is well known, there are different ways of solving such a system. In this paper, since we use a finite element method in which the pressure is continuous, we adopt the alternating direction strategy to compute $\mathbf{V}^{n+1}$ and p^{n+1}, as suggested in Reference 3, which we briefly recall.

After computing $\mathbf{X}^n$, we compute p^{n+1} by solving the Poisson equation

$$\nabla^2 p^{n+1} = \frac{1}{\Delta t}\operatorname{div}\mathbf{V}^n[\mathbf{X}^n(.; t)], \tag{16}$$

supplemented by Neumann-type non-homogeneous boundary conditions derived from the momentum equation. Finally we compute $\mathbf{V}^{n+1}$ by solving the first equation in (12).

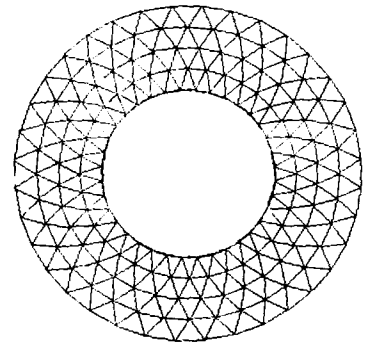

Figure 2. The mesh for test in a concentric problem

Table I. Results of test in a concentric problem

Re	AEV	REV	AEP	REP	ITE	Time
1	0·00183	0·000508	0·00244	0·00200	11	2·27
10	0·06040	0·018700	0·01710	0·01430	50	10·05
20	0·11630	0·036440	0·02651	0·02227	83	16·53
30	0·16560	0·052230	0·03430	0·02899	110	21·85
40	0·20910	0·066350	0·04090	0·03494	134	26·52
50	0·24810	0·079180	0·04696	0·04013	156	30·98

AEV—maximum absolute error for modulus of velocity.
REV—maximum relative error for modulus of velocity.
AEP—maximum absolute error for pressure.
REP—maximum relative error for pressure.
ITE—number of iterations needed.
Time—CPU time in minutes.

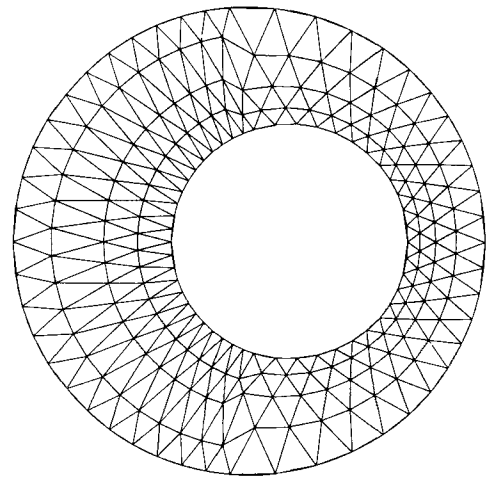

Figure 3. A typical mesh for an eccentric problem

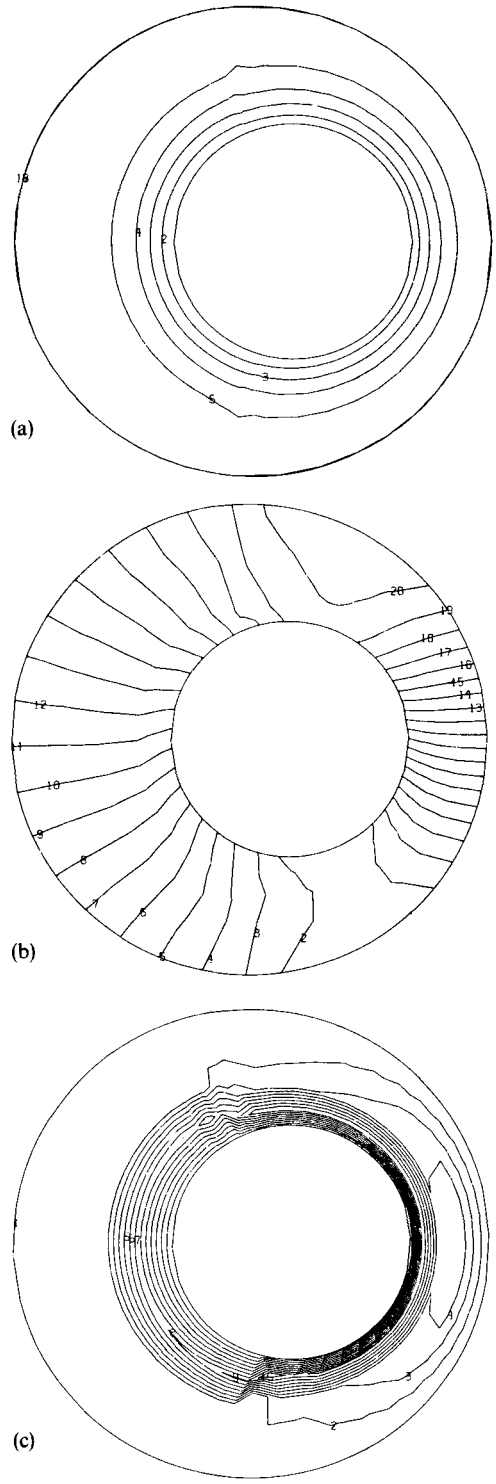

Figure 4. (a) Streamlines, (b) pressure contours and (c) isotherms for eccentricity 0·17 and $Re = 1$

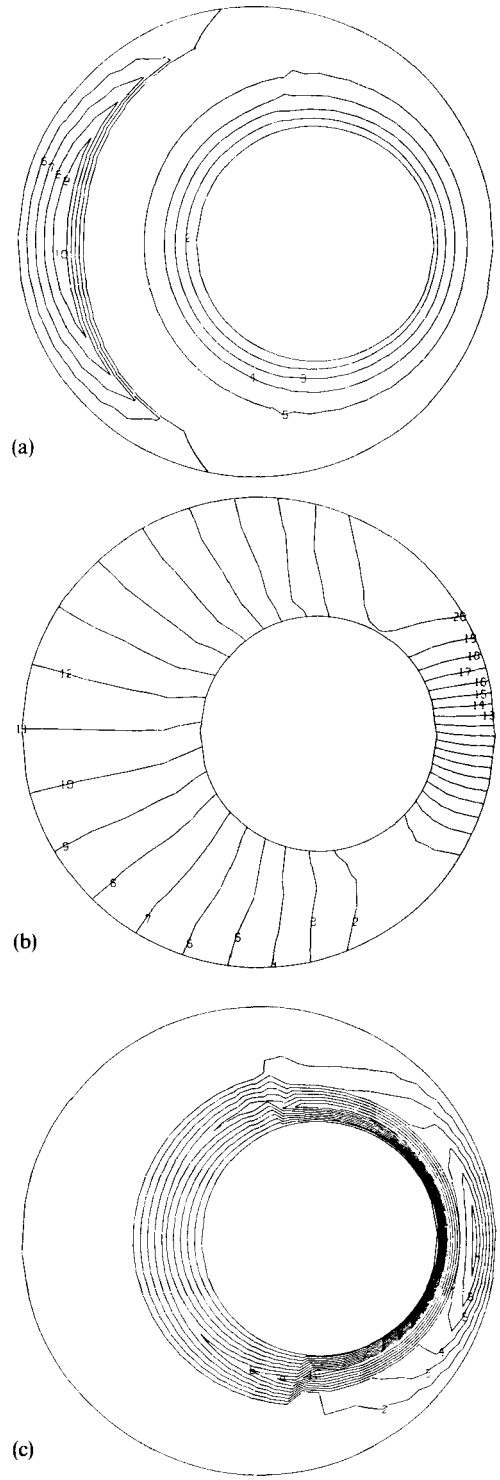

Figure 5. (a) Streamlines, (b) pressure contours and (c) isotherms for eccentricity 0·25 and $Re = 1$

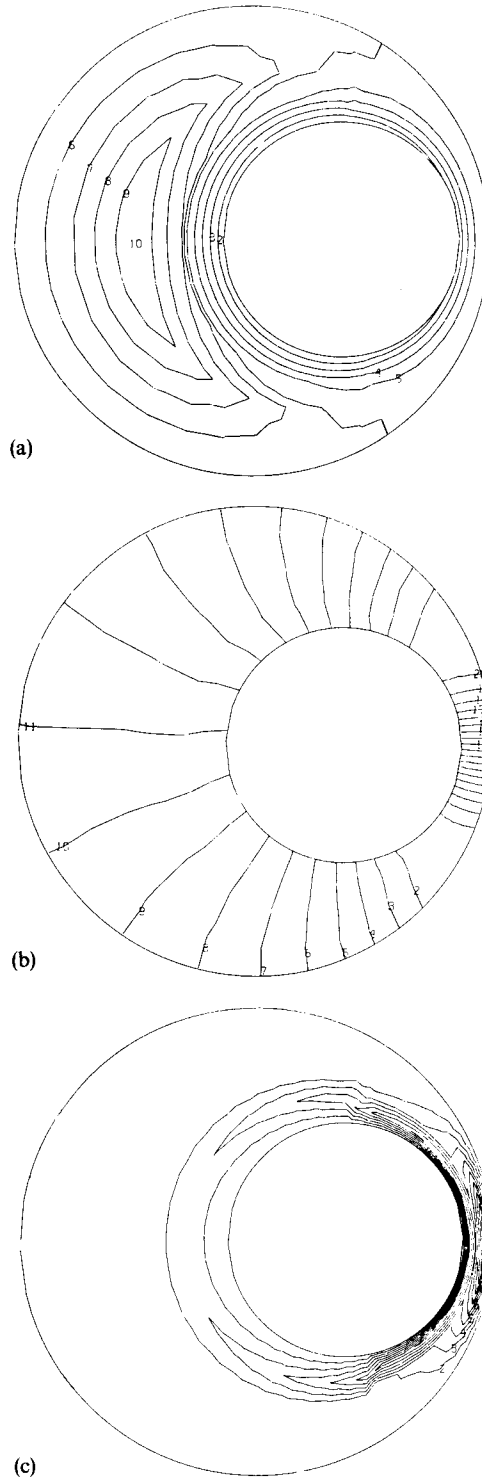

Figure 6. (a) Streamlines, (b) pressure contours and (c) isotherms for eccentricity 0·37 and $Re = 1$

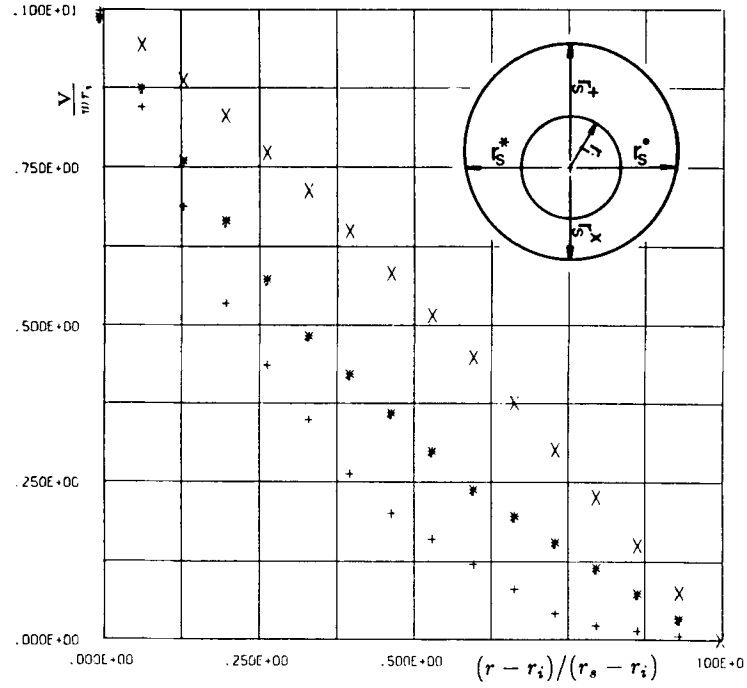

(a)

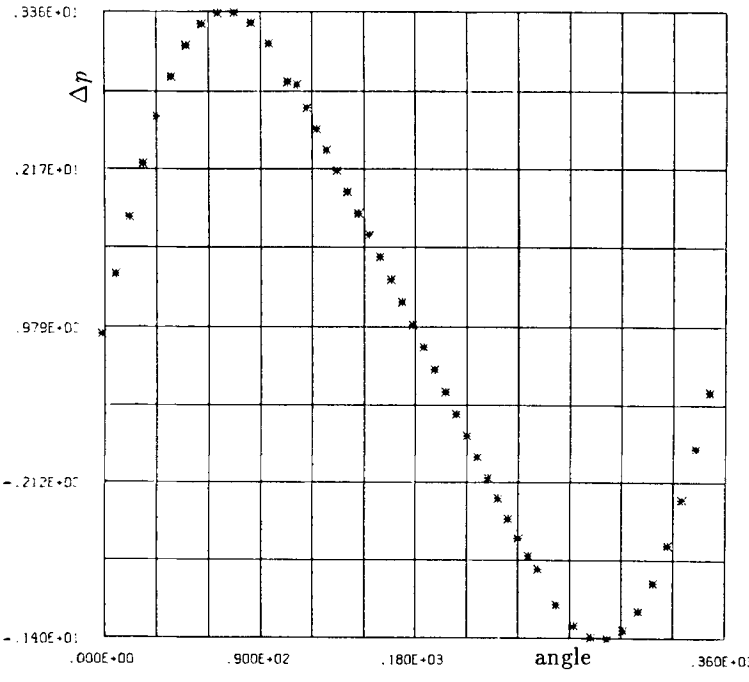

(b)

Figure 7. (a)–(b)

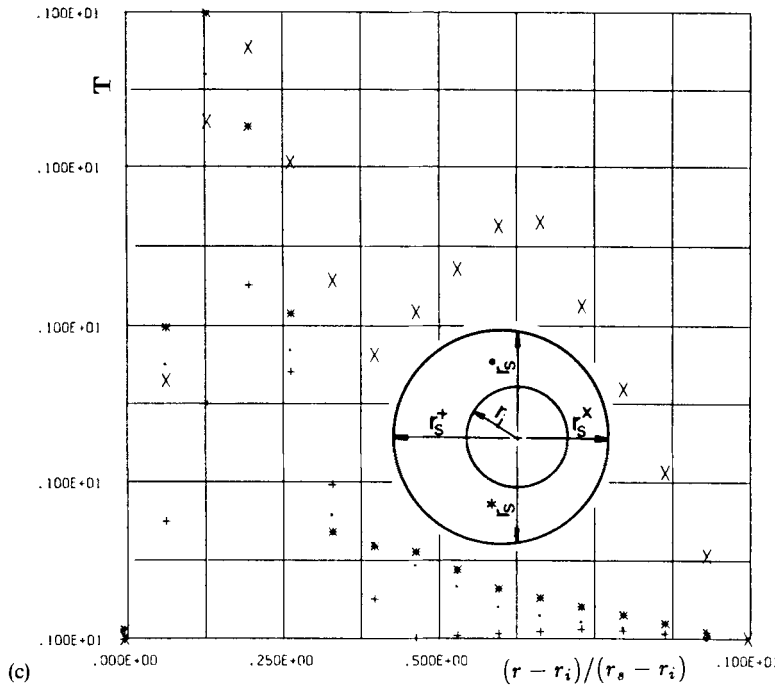

Figure 7. (a) Modulus of velocity, (b) pressure over inner cylinder and (c) temperature for eccentricity 0·17 and $Re = 1$

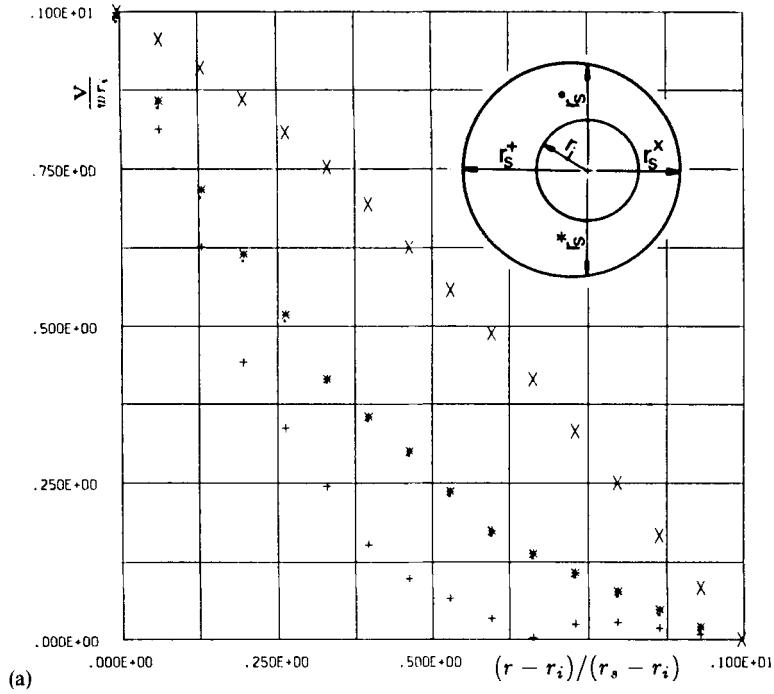

Figure 8. (a)

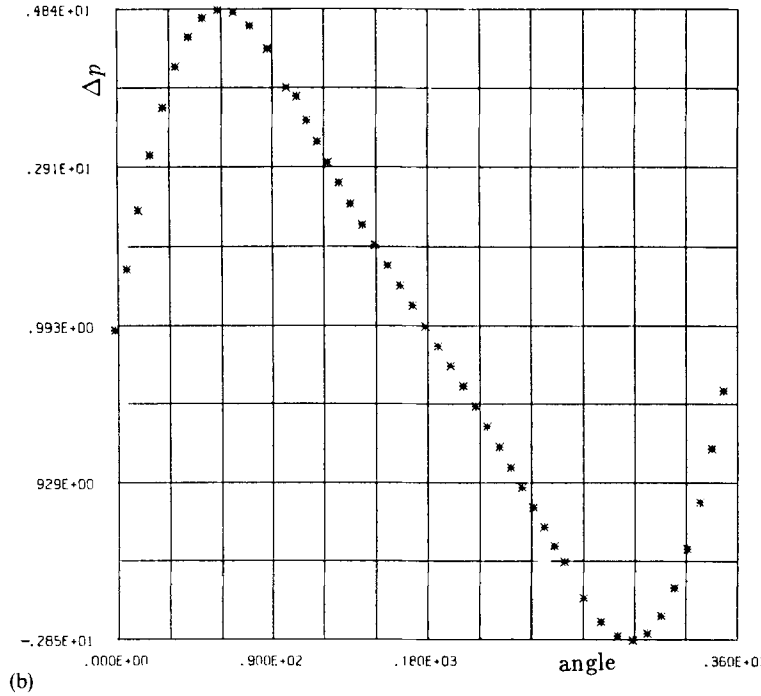

(b)

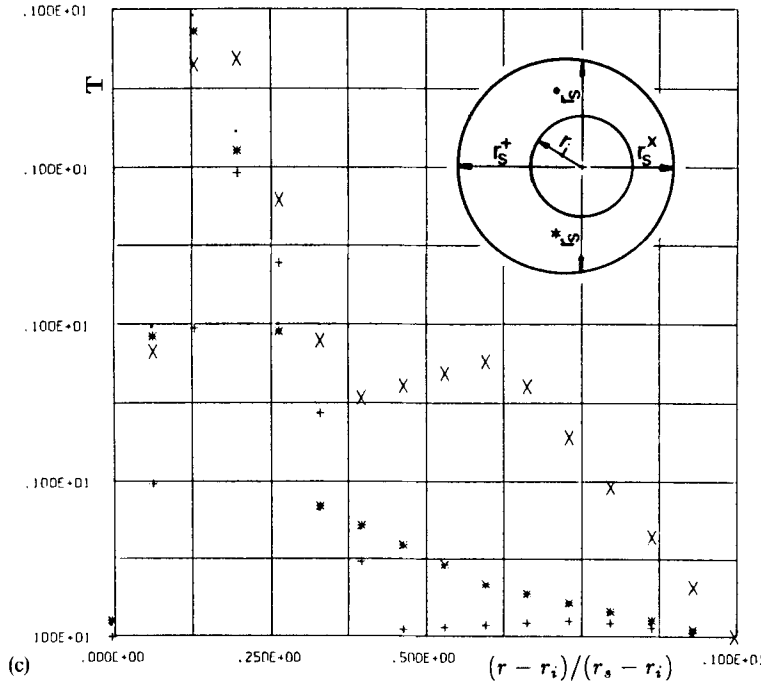

(c)

Figure 8. (a) Modulus of velocity, (b) pressure over inner cylinder and (c) temperature for eccentricity 0·25 and $Re = 1$

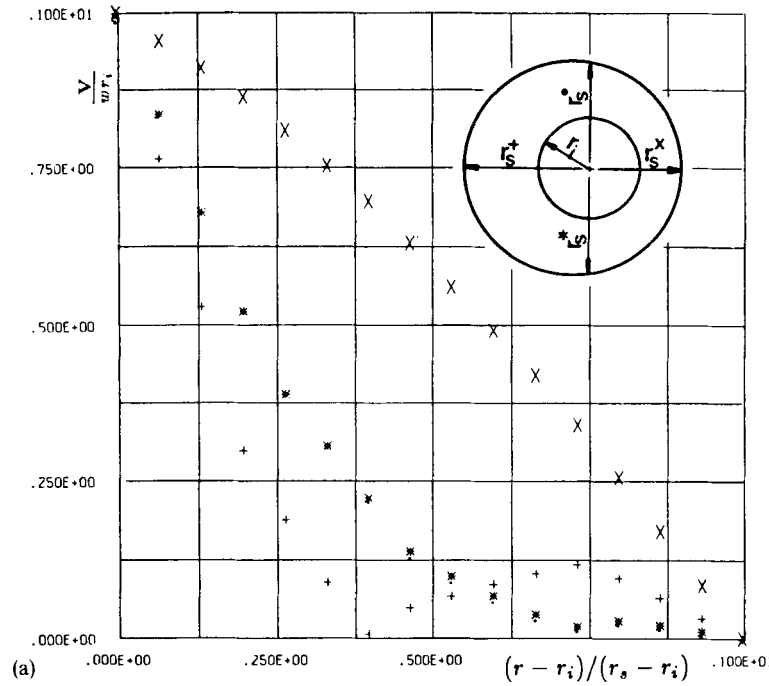
.100E+01
.750E+00
.500E+00
.250E+00
.000E+00
.000E+00
.250E+00
.500E+00
.100E+01
$(r - r_i)/(r_e - r_i)$
(a)

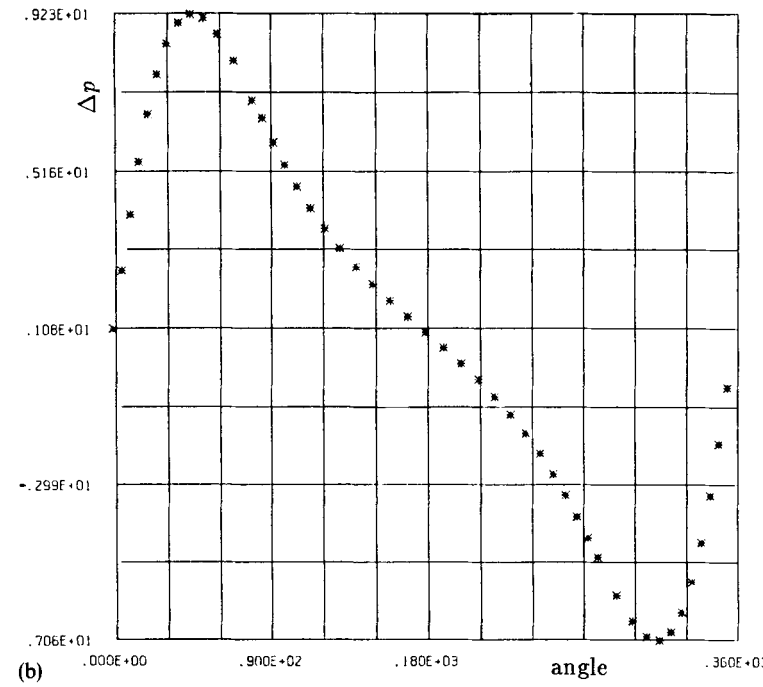
.923E+01
.516E+01
.108E+01
-.299E+01
.706E+01
Δp
.000E+00
.900E+02
.180E+03
.360E+03
angle
(b)

Figure 9. (a)–(b)

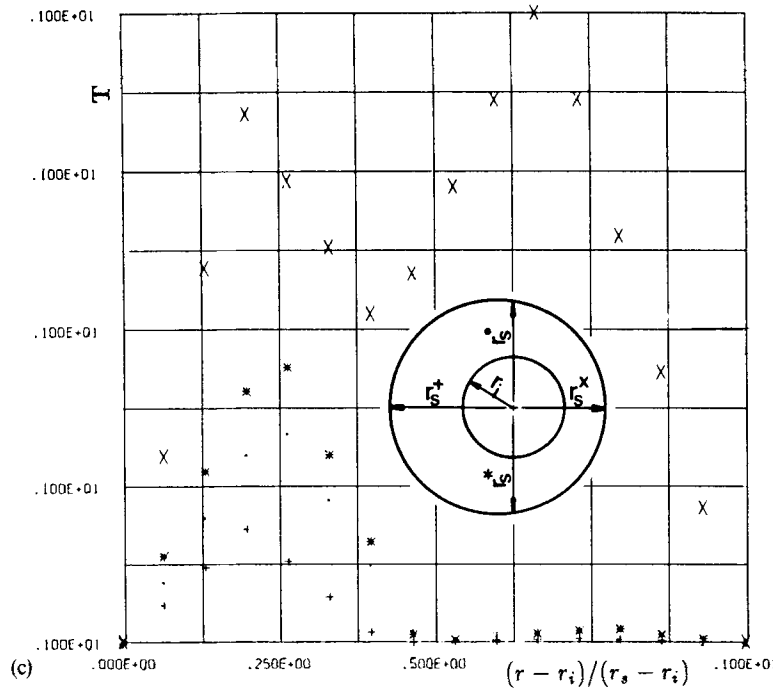

Figure 9. (a) Modulus of velocity, (b) pressure over inner cylinder and (c) temperature for eccentricity 0·37 and $Re = 1$

In order to discretize the resulting equations for $\mathbf{V}^{n+1}$, p^{n+1} and T^{n+1}, we use a mixed finite element method in which the pressure and the temperature are approximated by standard continuous piecewise linear functions defined on a triangular mesh, and the velocity is of the same type, though enriched by cubic functions that vanish on the boundary of the triangles. This kind of velocity approximation, first proposed in Reference 4, is aimed at stabilizing the pressure approximations while enabling a valid fulfilment of the incompressibility condition in an appropriate sense.[5]

4. RESULTS

In this section we show some representative numerical results obtained with a Fortran program, in which we codified the methodology described in the previous section. This code was run on a CYBER 170/835.

In order to check the accuracy of our numerical approach, we first solved problems whose exact solution is known, including an isotherm test problem. In this case an analytic solution can be easily constructed if one considers concentric cylinders as seen from the model problem given in Reference 6. This problem is among those that we used in our tests, in which we considered a ratio $r_e/r_i = 2$.

The resulting ring-shaped domain was subdivided into triangles in the manner illustrated in Figure 2. In the computations 288 elements were employed, thereby yielding 468 nodal points for the velocity and 180 nodal points for the pressure.

In Table I we give results obtained for Reynolds numbers ranging from 1 to 50. In the different columns we display absolute and relative errors for both velocity and pressure according to the

abbreviations indicated thereunder. Moreover, the number of iterations needed to attain a stationary flow for a maximum relative difference between the computed velocities at two consecutive time steps of 10^{-4}, for $\Delta t = 0{\cdot}1$, is given, together with the CPU time.

As one can infer from Table I, the results are rather satisfactory, although one observes a neat loss of accuracy as the Reynolds number increases.

Now we switch to the simulations performed for a completely eccentric model problem in which we kept $r_e/r_i = 2$. In all the computations a fixed mesh containing 384 elements was used, corresponding to 624 velocity nodal points and 240 pressure nodal points. A typical mesh is illustrated in Figure 3 for an eccentricity of 0·17.

The tolerance for the maximum absolute error between the velocities in consecutive time steps is again 10^{-4}, but this time we chose $\Delta t = 0{\cdot}01$.

The physical constants defining the viscosity are $A = 2{\cdot}427 \times 10^{-10}$ and $B = 6605{\cdot}547$, while the Prandtl number equals 29×10^3.

First we took $Re = 1$ and three different values of the eccentricity, namely 0·17, 0·25 and 0·37. For each of these values we display in Figures 4–6 (a) the streamlines, (b) the pressure contours and (c) the isotherms. In Figures 7–9 we show (a) the modulus of the velocity, (b) the pressure and (c) the temperature along different sections of the domain specified in the figures, together with the corresponding notation.

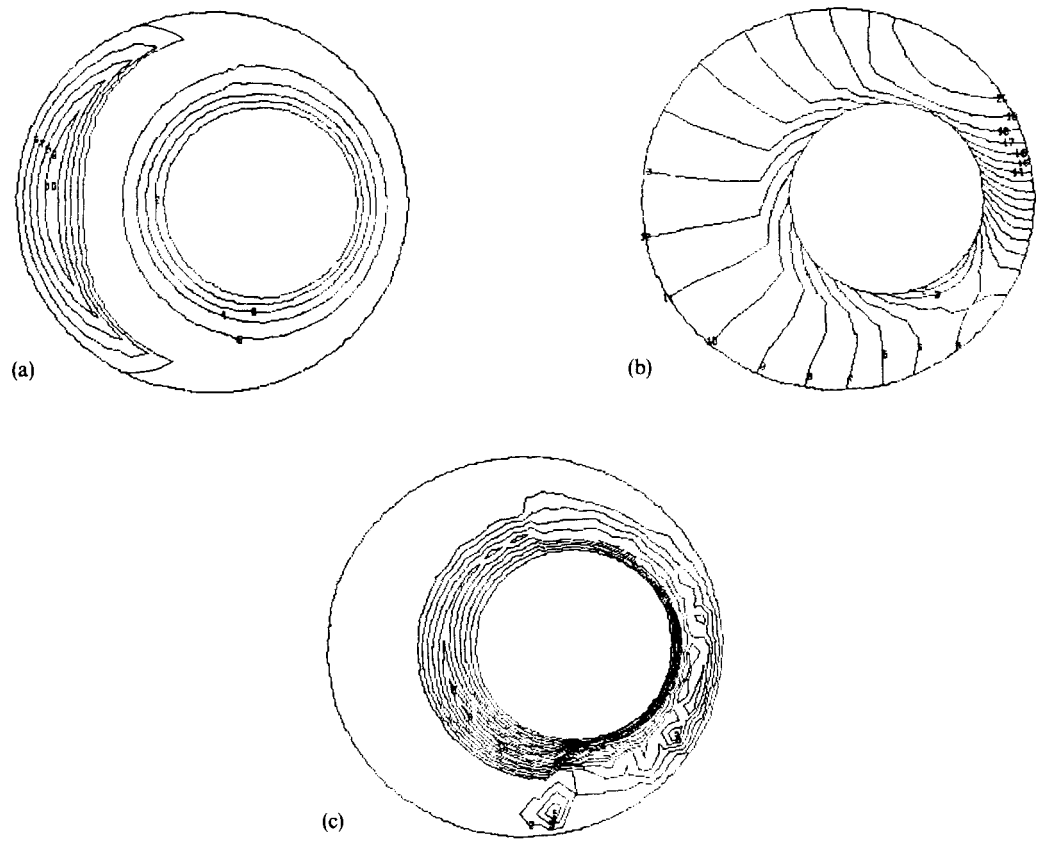

Figure 10. (a) Streamlines, (b) pressure contours and (c) isotherms for eccentricity 0·25 and $Re = 10$

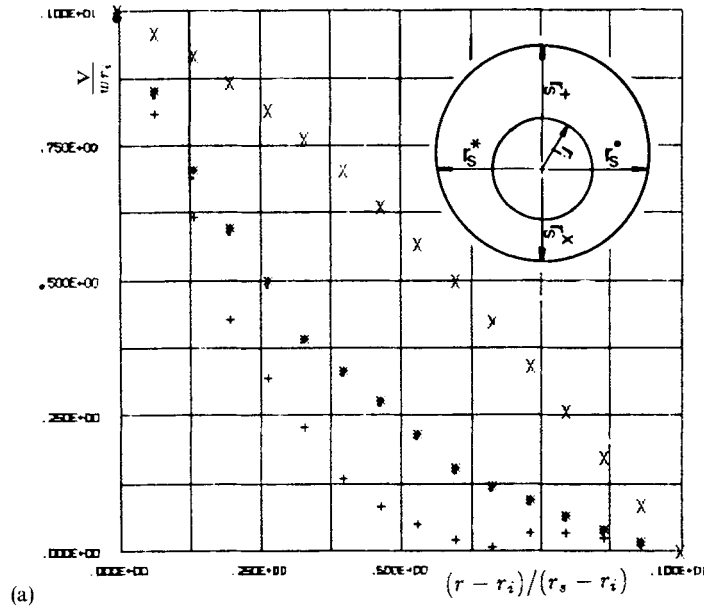

(a)

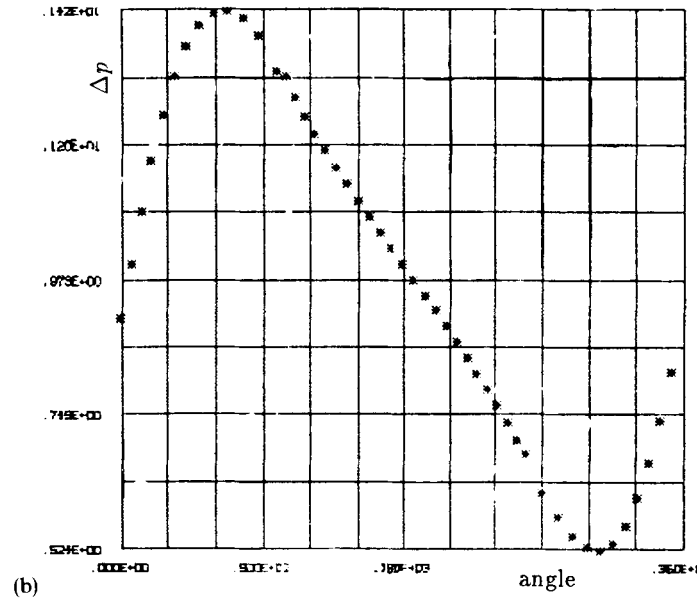

(b)

Figure 11. (a)–(b)

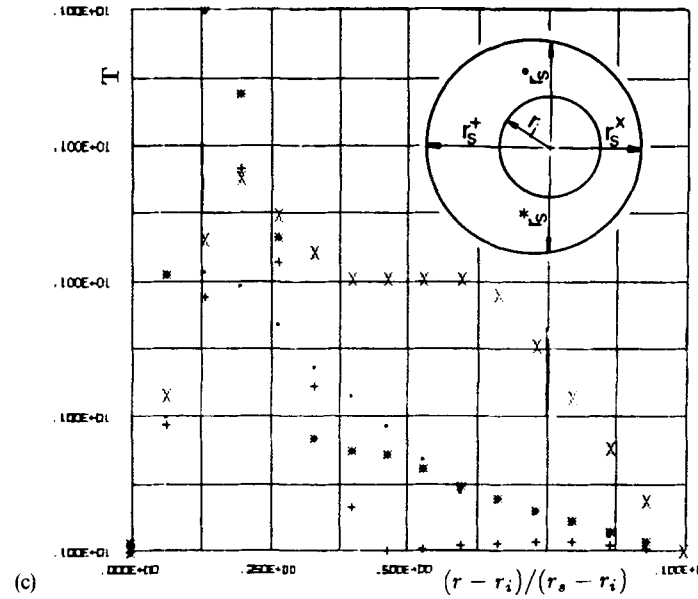

(c)

Figure 11. (a) Modulus of velocity, (b) pressure over inner cylinder and (c) temperature for eccentricity 0·25 and $Re = 1$

Some conclusions can be drawn in the light of the above results, among which are the following.

(i) The pressure profile on the inner cylinder is symmetric with respect to the horizontal axis; this effect had been predicted by Andres and Szari.[7]
(ii) The effect of the pressure gradient in the narrowest part of the flow domain tends to give a concave aspect to the streamlines.
(iii) The temperature profiles are realistic and show quite a good qualitative agreement with results obtained for concentric cases using one-dimensional model.[8]

Next we considered a fixed eccentricity of 0·25 and changed the Reynolds number to 10. In Figures 10 and 11 we show analogous results to Figures 4–6 and 7–9 respectively.

It is interesting to observe that the total variation of the pressure on the inner cylinder increases significantly. This effect could be predicted, since the inertia of the fluid increases with the Reynolds number.

5. CONCLUSIONS

The main goals of this work were attained, since an efficient finite element model of the viscous flow of a Newtonian fluid with viscosity depending on the temperature was derived according to the numerical results given above.

However, the need to work with finer meshes than those we used in the computations described in this paper appeared clearly. In order to cope with this difficulty, we are presently improving the solution of linear systems by implementing standard solvers with less storage requirements. We hope to be able to report these finer results with the resulting optimized code in the near future.

REFERENCES

1. G. I. Taylor, 'Stability of viscous liquid contained between two rotating cylinders', *Phil. Trans. R. Soc. Ser. A*, **223,** 289–343 (1923).
2. O. Pironneau, 'On the transport–diffusion algorithm and its applications to the Navier–Stokes equations', *Numer. Math.*, **38,** 309–332 (1982).
3. J. P. Huffenus and D. Khaletzky, 'The lagrangian approach of advective term treatment and its application to the solution of Navier–Stokes equation' *Int. j. numer. methods fluids*, **1,** 365–387 (1981).
4. V. Ruas, 'Sur l'application de quelques méthodes d'éléments finis à la résolution d'un probleme d'élasticité incompressible non linéaire', *Rapport de Recherche 24*, INRIA, Rocquencourt, France, 1980.
5. D. N. Arnold, F. Brezzi and M. Fortin, 'A stable finite element for the Stokes equations', *Calcolo*, **21-4,** 337–344 (1984).
6. H. Schlichting, *Boundary-Layer Theory*, McGraw-Hill, New York, 1979.
7. A. S. Andres and A. Z. Szeri, 'Flow between eccentric rotating cylinders', *J. Appl. Mech.*, **51,** 869–878 (1984).
8. J. H. C. Araujo, 'Simulações numéricas via elementos finitos de escoamentos viscosos entre cilindros concêntricos e excêntricos com interno girante e viscosidade variável', *Dissertação de Mestrado*, Departamento de Engenharia Mecânica, PUC/RJ, 1987.